Fast and Slow Responses of Equatorial SST Pattern to CO_2 Forcing

Kezhou Lu (kezhou.lu@eas.gatech.edu) and **Jie He**

Motivations

- The long-term responses of equatorial Pacific sea surface temperature (SST) pattern to anthropogenic forcing has long been studied, but little is known about how much CO_2 effect contributes to these changes during a short time period.
- Abrupt 4xCO_2 experiment is used to emphasize the effect of CO_2 during a global warming process. This effect happens within the first few years, and the internal variability poses a big challenge in assessing the significance of CO_2 forced changes.
- The role of air-sea coupling during a short time period after imposing CO_2 needs to be better understood.

Highlights

Important results:

- An initial cooling pattern is found in Equatorial Pacific during fast response period.
- Strengthening in most of the equatorial atmospheric circulation in the first 2 years.

Model and experiment setup[1]:

- A very large initial ensemble abrupt 4xCO_2 experiment of CESM1 is used in order to eliminate internal variability.

Define fast and slow responses

Fast responses:

- First 2 years of fully coupled abrupt 4xCO_2 simulation is chosen because equatorial shows a rapid change in this period
- Including both direct CO_2 forcing (important within the first month) rapid land-sea contrast and air-sea coupling

Slow responses:

- Last 30 years of the simulation (89-119 years in this research)
- The earth system reaches equilibrium in this time period

Goal

- Explore the development of this fast cooling pattern and it's evolution into an enhanced equatorial warming pattern.
- Compare the equatorial atmospheric circulation between fast and slow responses periods

- Pre-industrial Control: 0-160 years
- 4xCO_2 ensemble members branch off from different years as indicated below:

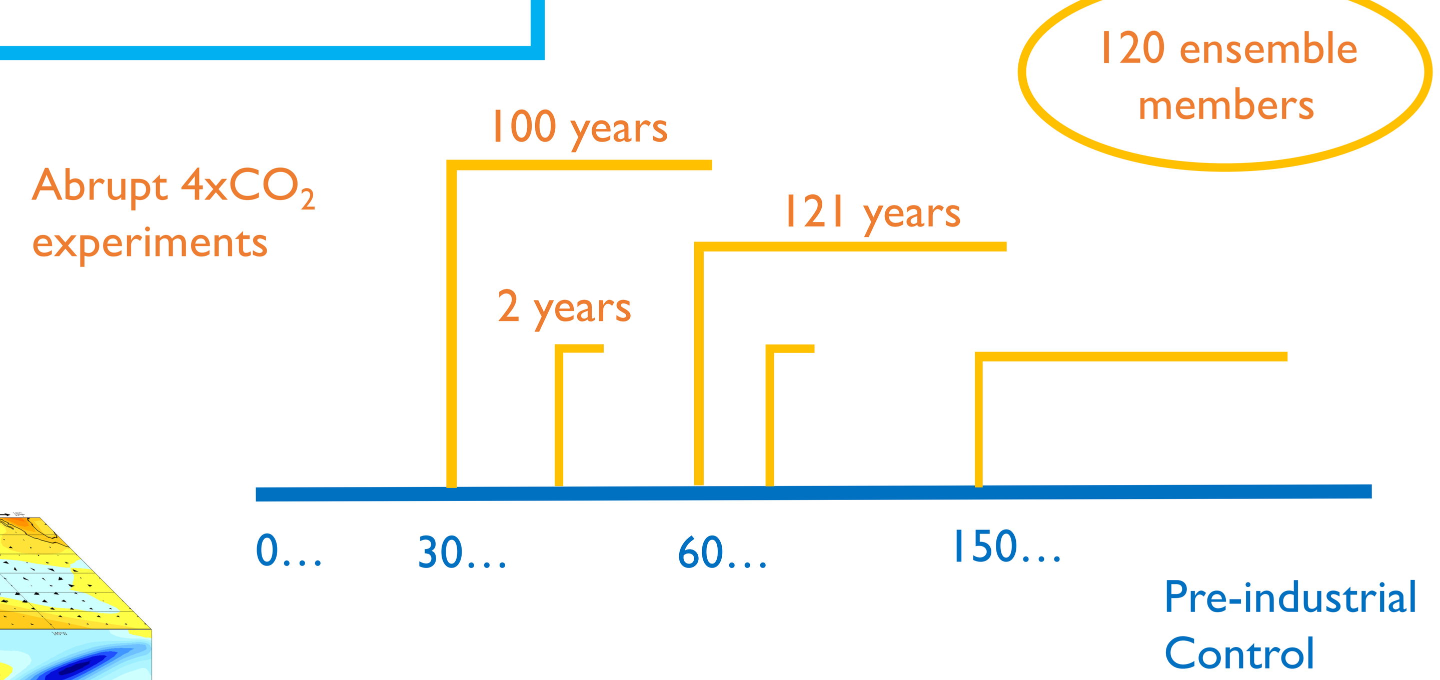

Fast responses

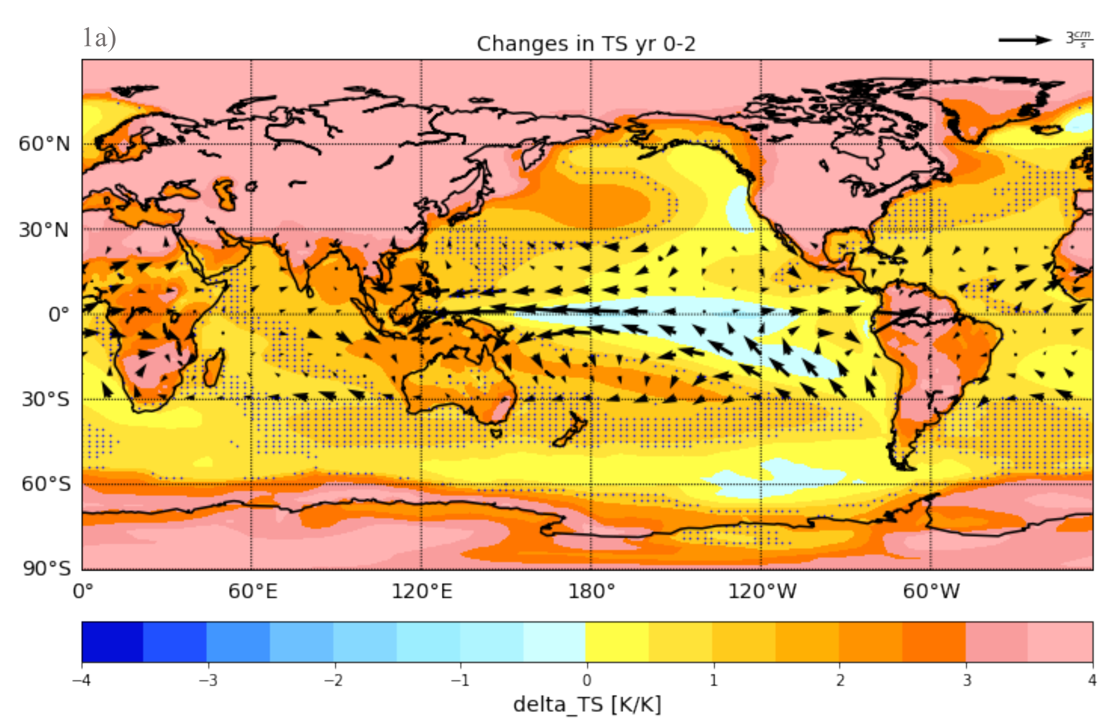

Changes of surface temperature in the first 2 years normalized by global mean temperature changes (shadings) and equatorial surface wind anomalies(vectors) between 4xCO_2 and pre-industrial control. Stippling indicates regions which are dominated by internal variability, based on Monte-Carlo simulation of sea surface temperature[2].

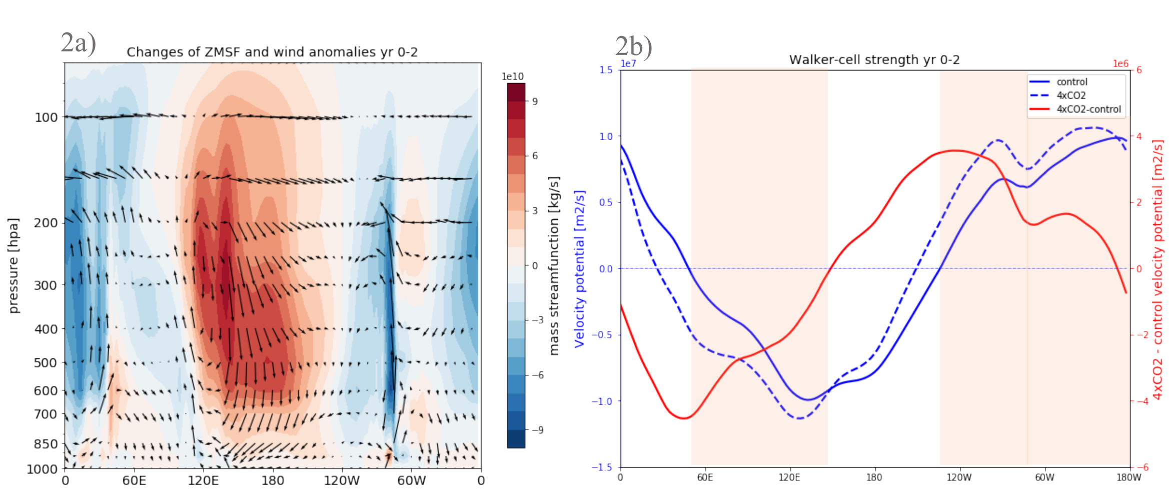

Left: changes of zonal mean mass stream functions (shadings) and vertical wind anomalies (vectors) averaged over 5°S to 5°N between 4xCO_2 and pre-industrial control. Right: Walker-cell strength calculated by averaging 40°S to 40°N 200 hpa velocity potential. The orange shading indicates regions with a strengthening of Walker circulation. Results shown here are averaged over the first 2 years of simulations.

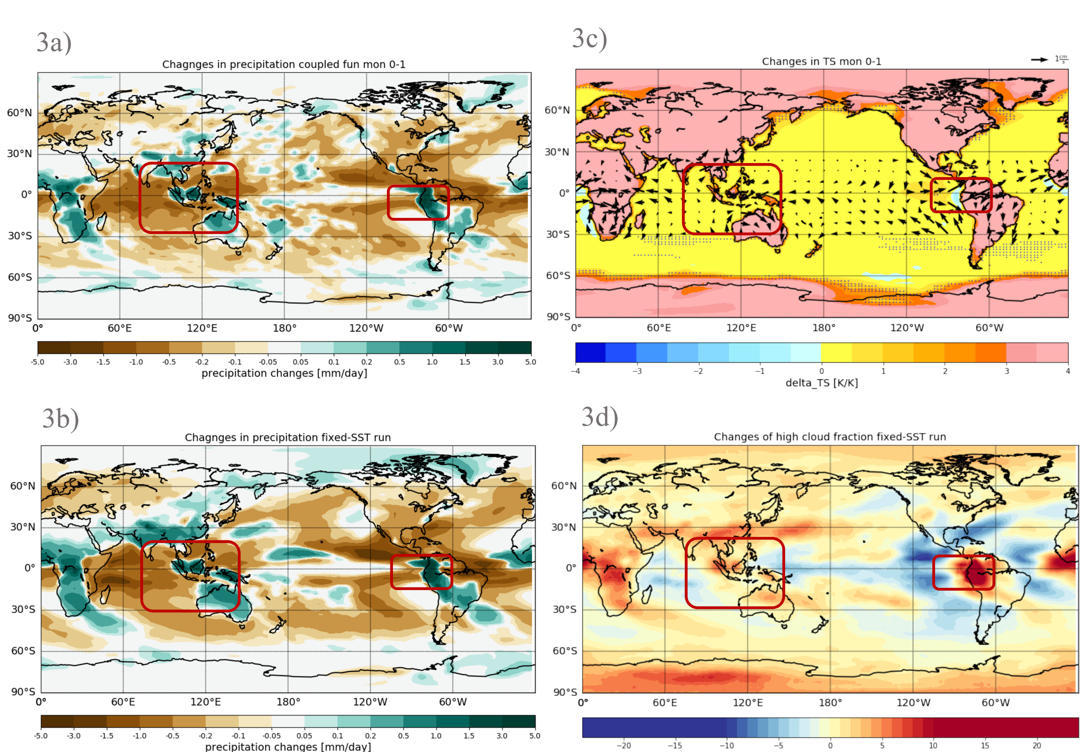

Left column: Changes of precipitation between 4xCO_2 and pre-industrial control. 3c) Same as 1a) but for the results of the first month after abrupt 4xCO_2. 3d) Changes of high cloud fraction. The upper row shows results of the first month after abrupt 4xCO_2 from fully coupled large ensemble mean, and the bottom row shows results averaged over 30 years of fixed-SST simulation.

- Direct CO_2 forcing together with land-sea contrast lead to wind anomalies and strong upward motion near coast (regions boxed in red in figure 3).
- Strong westward anomalies keep piling up warm water in the western equatorial Pacific
- Strengthening in part of the Walker Circulation(figure 2b).

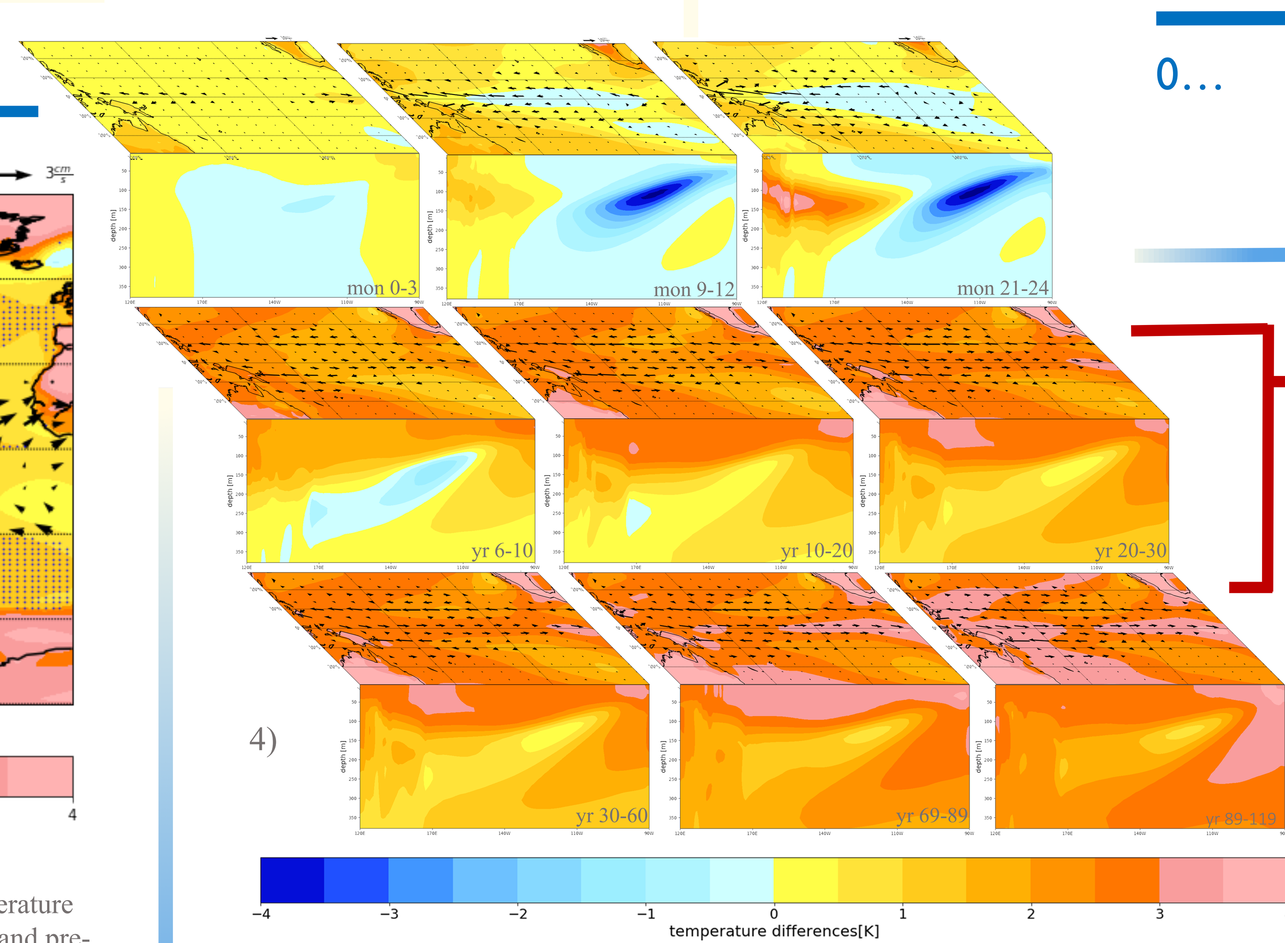

Time evolution of surface (horizontal) and subsurface (vertical, averaged from 2°S to 2°N) temperature differences (shadings) and surface ocean current at 5m depth (vectors).

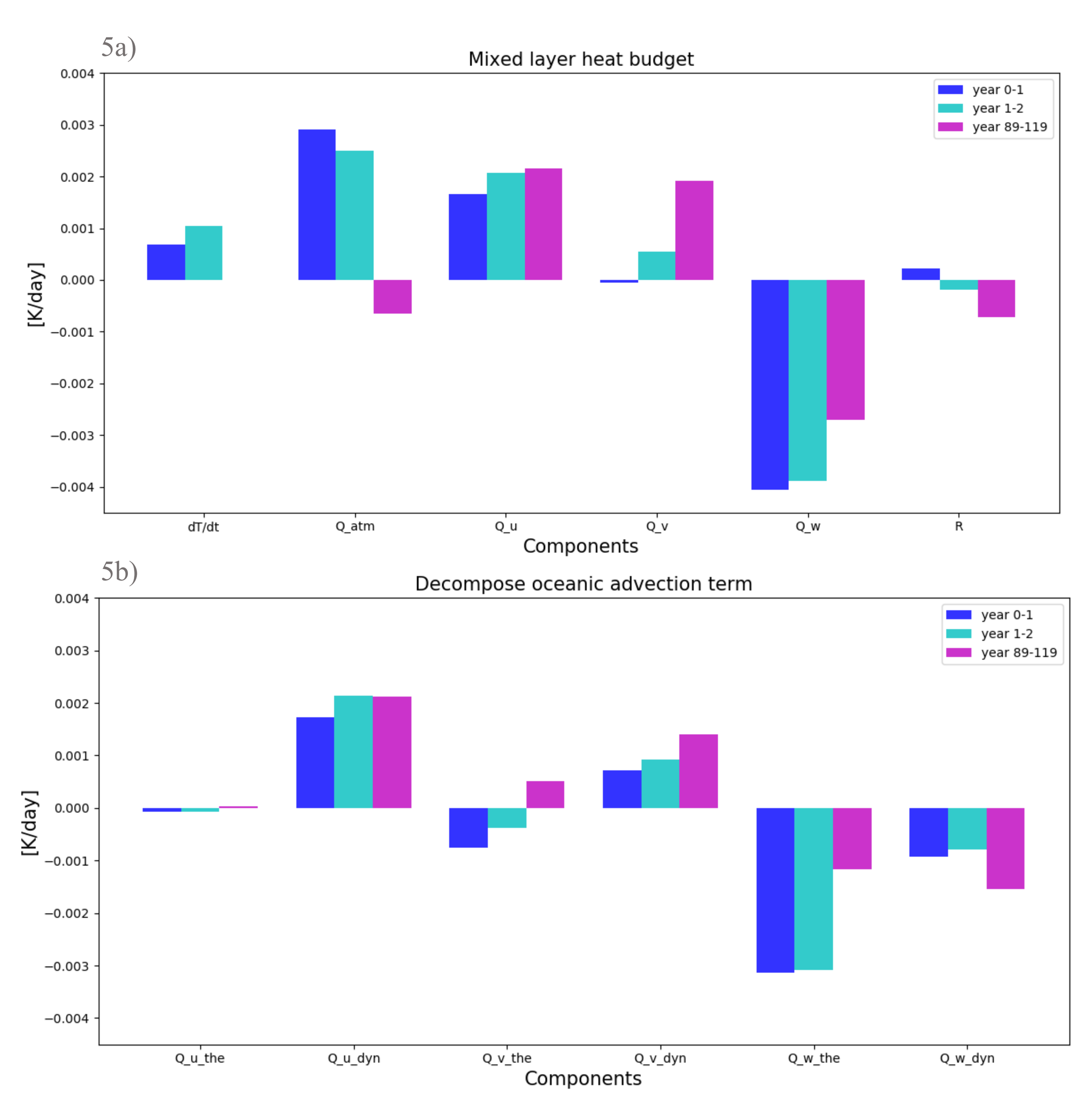

Top: mixed layer heat budget with mixed layer depth h_m= 75m, averaged over 170°W-90°W for the first, second and last 30 years. Bottom: Decompose zonal, meridional and vertical advection terms in (5a) into dynamical and thermodynamic components [3].

$$Q_{atm} = \frac{(SW + LW - SH - LH)}{\rho_0 c_p h_m}$$

$$Q_u = -\frac{1}{h_m}\int_0^{h_m} u\frac{\partial T}{\partial x}dz$$

$$Q_w = -\frac{1}{h_m}\int_0^{h_m} w\frac{\partial T}{\partial z}dz$$

$$Q_v = -\frac{1}{h_m}\int_0^{h_m} v\frac{\partial T}{\partial y}dz$$

$$R = {dT}/{dt} - Q_{atm} - Q_u - Q_v - Q_w$$

$$Q_{u_{dyn}} = -\frac{1}{h_m}\int_0^{h_m} u'\frac{\partial \bar{T}}{\partial z}dz$$

$$Q_{u_{the}} = -\frac{1}{h_m}\int_0^{h_m} \bar{u}\frac{\partial T'}{\partial z}dz$$

$$Q_{v_{dyn}} = -\frac{1}{h_m}\int_0^{h_m} v'\frac{\partial \bar{T}}{\partial z}dz$$

$$Q_{v_{the}} = -\frac{1}{h_m}\int_0^{h_m} \bar{v}\frac{\partial T'}{\partial z}dz$$

$$Q_{w_{the}} = -\frac{1}{h_m}\int_0^{h_m} \bar{w}\frac{\partial T'}{\partial z}dz$$

$$Q_{w_{dyn}} = -\frac{1}{h_m}\int_0^{h_m} w'\frac{\partial \bar{T}}{\partial z}dz$$

Summary

- Wind anomalies triggered by land-sea contrast together with ocean dynamics develop the fast cooling pattern.
- The weakening of anomalous easterlies and smoothing of vertical temperature gradient turn fast cooling to slow warming pattern.

Slow responses

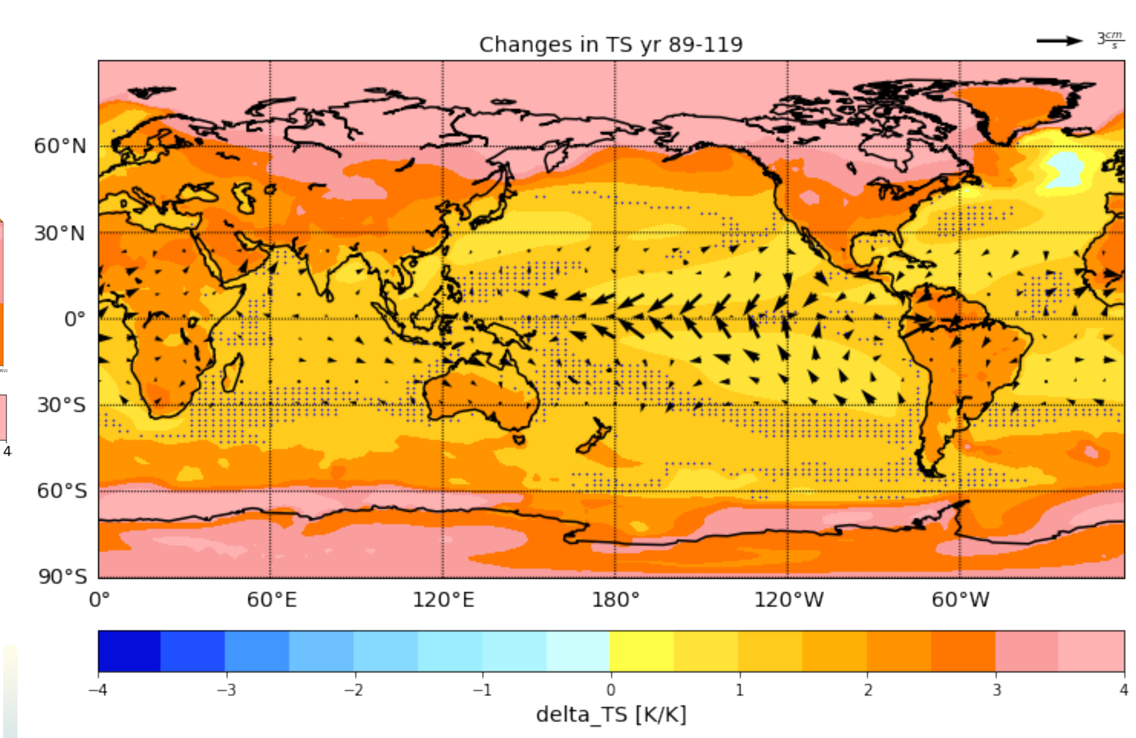

Changes of surface temperature in the last 30 years normalized by global mean temperature changes (shadings) and equatorial surface wind anomalies(vectors) between 4xCO_2 and pre-industrial control simulation. Stippling indicates regions which are dominated by internal variability, based on Monte-Carlo simulation of sea surface temperature[2].

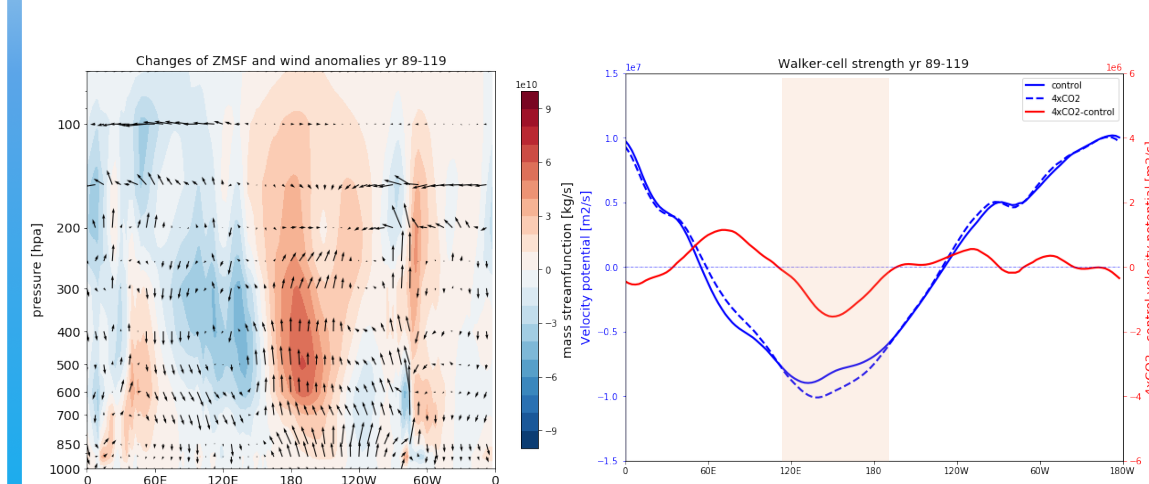

Left: changes of zonal mean mass stream functions (shadings) and vertical wind anomalies (vectors) averaged over 5°S to 5°N between 4xCO_2 and pre-industrial control. Right: Walker-cell strength calculated by averaging 40°S to 40°N 200 hpa velocity potential. The orange shading indicates regions with a strengthening of Walker circulation. Results shown here are averaged over the last 30 years of simulations.

- Anomalous easterlies become almost zero
- Downwelling oceanic Kelvin wave transports warm water from west to east
- The magnitude of vertical ocean temperature gradient $\left|\frac{\partial T'}{\partial z}\right|$ keeps decreasing
- Forms an enhanced equatorial warming pattern

References

[1] Rugenstein, M. A. A., J. M. Gregory, N. Schaller, J. Sedláček, and R. Knutti, 2016: Multiannual Ocean–Atmosphere Adjustments to Radiative Forcing. Journal of Climate, 29, 5643-5659.
[2] Zhang, H., and T. L. Delworth, 2018: Robustness of anthropogenically forced decadal precipitation changes projected for the 21st century. Nat Commun, 9, 1150.
[3] DiNezio, P. N., A. C. Clement, G. A. Vecchi, B. J. Soden, B. P. Kirtman, and S.-K. Lee, 2009: Climate Response of the Equatorial Pacific to Global Warming. Journal of Climate, 22, 4873-4892.

Acknowledgements

I would like to thank my advisor Dr. Jie He , who supervised me for this project. I also would love to thank Dr. Maria Rugenstein, who provided me with both the large ensemble data and a lot of good suggestions.

Fast and Slow Responses of Equatorial SST Pattern to CO_2 Forcing

Kezhou Lu (kezhou.lu@eas.gatech.edu) and **Jie He**

Georgia Tech

Define *Fast* and *Slow* Responses Time Periods

Fast responses:

- First 2 years of fully coupled abrupt $4xCO_2$ simulation
- Including both direct CO_2 forcing (important within the first month) and air-sea coupling

Slow responses:

- Last 30 years of the simulation (89-119 years in this research)

Highlights

Model and experiment setup:

- A very large initial ensemble abrupt $4xCO_2$ experiment of CESM1 is used, in order to eliminate internal variability[1].

Important results:

- A "*La Niña*-Like" initial cooling pattern is found in Equatorial Pacific during fast response period.
- Strengthening of Equatorial atmospheric circulation in the first 2 years.

Goal

Explore the development of this "*La Niña*-Like" fast cooling pattern and it's evolution into an "*El Niño*-Like" slow warming pattern.

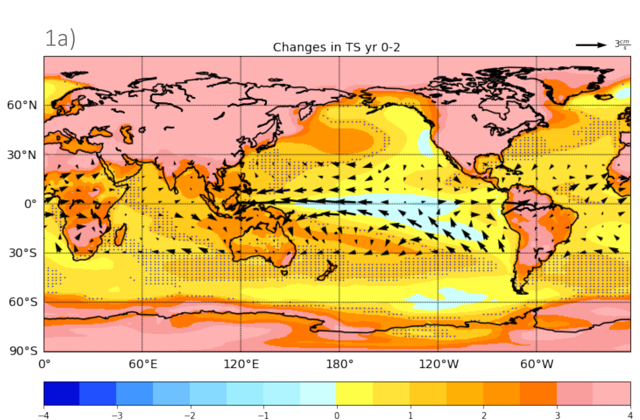

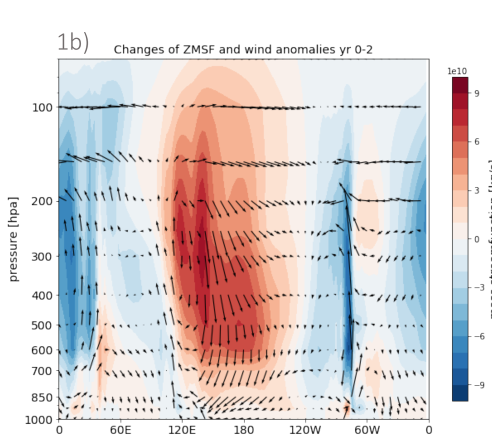

1a) & 1c): Changes of surface temperature normalized by global mean temperature changes (shadings) and equatorial surface wind anomalies(vectors) between $4xCO_2$ and pre-industrial control simulation. Stippling indicates regions which are dominated by internal variability, based on Monte-Carlo simulation.

Fast responses

Fast Responses

3a)

$$Q_{atm} = \frac{SW + LW - SH - LH}{\rho_0 c_p h_m}$$

3c)

$$Q_u = -\frac{1}{h_m}\int_0^{h_m} u\frac{\partial T}{\partial x}dz$$

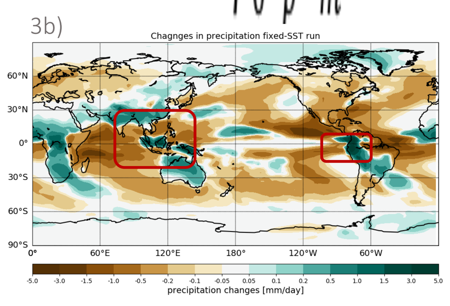

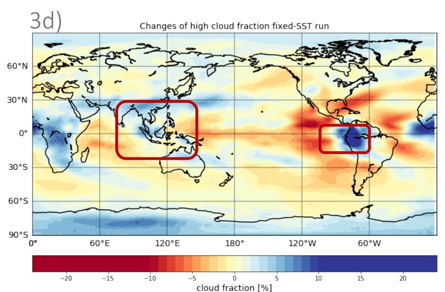

3a) & 3b): Changes of precipitation. **3c)** Same as 1a) but for the results of the first month after abrupt $4xCO_2$. **3d)** Changes of high cloud fraction. **3a) & 3c)** Results from fully coupled run in the first month after abrupt $4xCO_2$. **3b) & 3d)** Results from 30 years of fixed-SST simulation.

- Direct CO_2 forcing together with land-sea contract lead to wind anomalies and strong upward motion near coast (regions boxed in red)

Slow Responses

- Anomalous easterlies become almost zero
- Downwelling oceanic kelvin wave transports warm water from west to east
- The magnitude of vertical ocean temperature gradient $\left|\frac{\partial T'}{\partial z}\right|$ keeps decreasing
- Forms "*El Niño*-Like" warming pattern

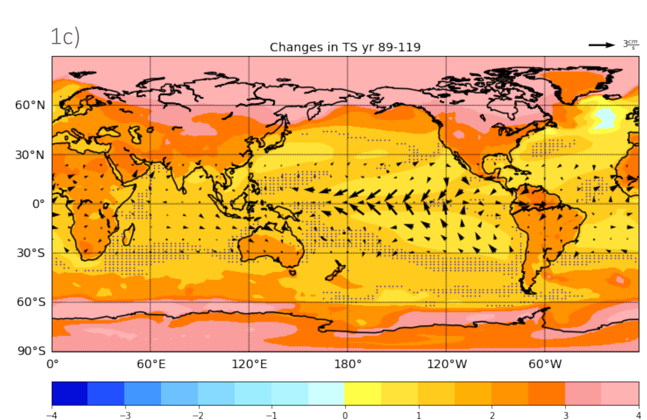

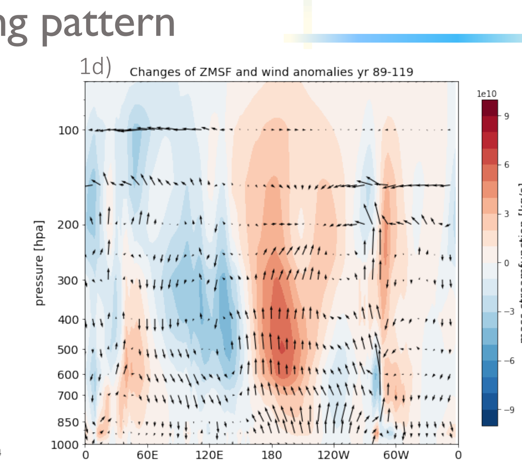

1b) & 1d): Changes of zonal mean mass stream functions (shadings) and vertical wind anomalies (vectors) averaged over 5°S to 5°N between $4xCO_2$ and pre-industrial control. The first 2-year average for (b) and last 30-year average for (d).

Slow responses

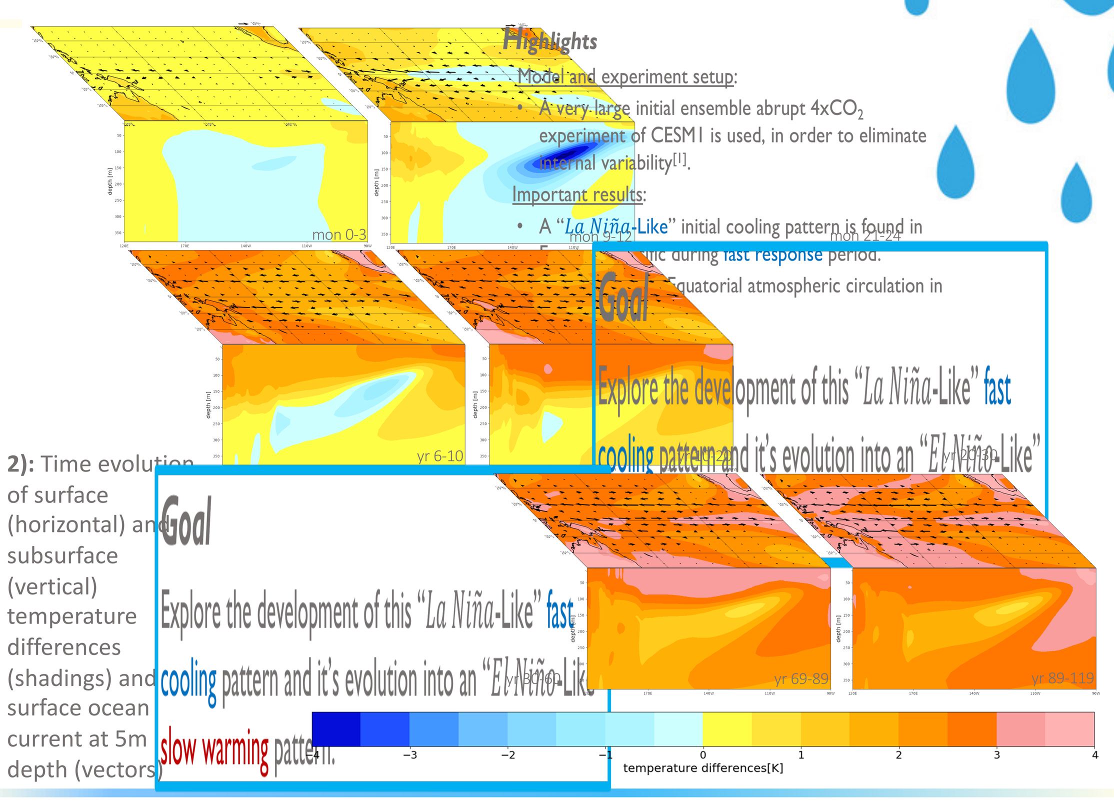

2): Time evolution of surface (horizontal) and subsurface (vertical) temperature differences (shadings) and surface ocean current at 5m depth (vectors)

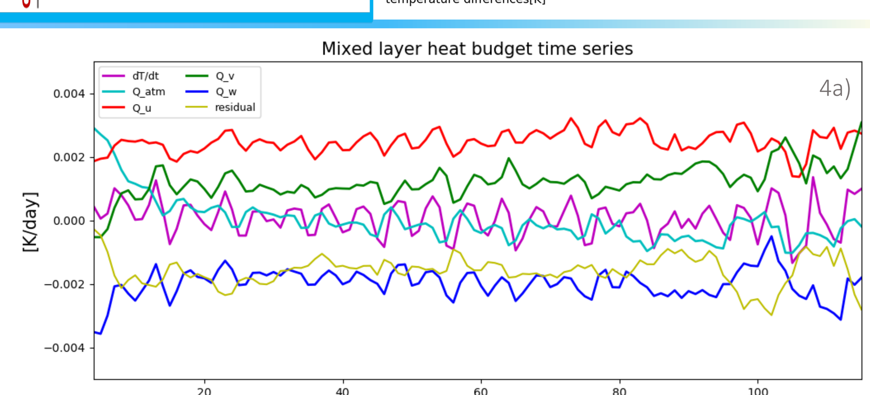

4a): Mixed layer heat budget with depth h_m=75m, averaged over 170°W-90°W

$$Q_u = -\frac{1}{h_m}\int_0^{h_m} u\frac{\partial T}{\partial x}dz$$

$$Q_v = -\frac{1}{h_m}\int_0^{h_m} v\frac{\partial T}{\partial y}dz$$

$$Q_w = -\frac{1}{h_m}\int_0^{h_m} w\frac{\partial T}{\partial z}dz$$

$$Q_{atm} = \frac{(SW + LW - SH - LH)}{\rho_0 c_p h_m}$$

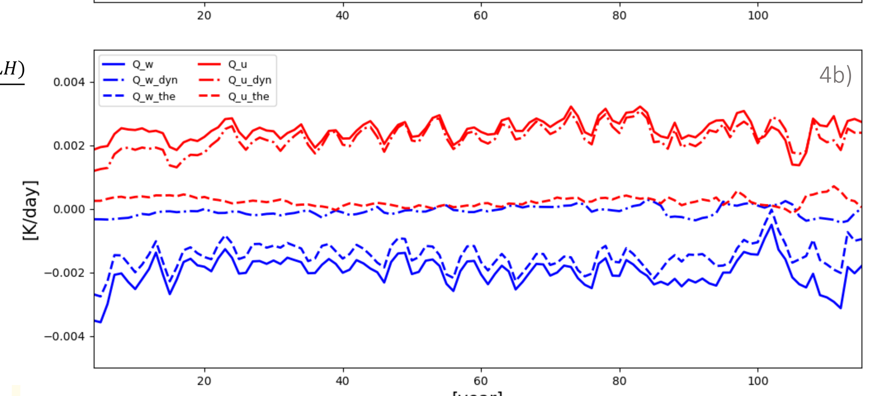

4b): Decompose zonal and vertical advection terms into dynamical and thermodynamical components

$$Q_{w_{dyn}} = -\frac{1}{h_m}\int_0^{h_m} w'\frac{\partial \bar{T}}{\partial z}dz \;;\; Q_{w_{the}} = -\frac{1}{h_m}\int_0^{h_m} \bar{w}\frac{\partial T'}{\partial z}dz$$

Same for $Q_{u_{dyn}}$ and $Q_{u_{the}}$

Summary

- Wind anomalies triggered by land-sea contract together with ocean dynamics develop the fast cooling pattern.
- The weakening of anomalous easterlies and smoothing of vertical temperature gradient turn fast cooling to slow warming pattern.

References:

[1] Rugenstein, M. A. A., J. M. Gregory, N. Schaller, J. Sedláček, and R. Knutti, 2016: Multiannual Ocean–Atmosphere Adjustments to Radiative Forcing.